A Multifunctional Pipette

Alar Ainla,* Gavin D. M. Jeffries, Ralf Brune, Owe Orwar and Aldo Jesorka

Electronic Supplementary Information (ESI)

Table of contents

Supplementary methods

Fabrication

Microchannel mold. All microchannel molds were prepared in the ISO100 cleanroom facility MC2 at Chalmers University of Technology. In order to yield ~20 µm thick SU-8 structures, SU-8-10 was dispensed onto 4" wafer and spun for 30 s at 1600 rpm (acceleration: 5 s till 500 rpm and 4 s till 1600 rpm), followed by baking for 2.5 min at 65 °C and 6 min at 95 °C. Thereafter the resist was exposed (200 mJ/cm^2) through a chromium mask in a Karl Süss MA6 contact mask aligner (G-line, 5-6 mW/cm^2), post baked for 1 min at 65 °C and 3 min at 95 °C and developed for 4 min in SU-8 developer (1-methoxy-2-propyl acetate). Finally the molds were cleaned by spraying with isopropanol and water, blow dried, ashed in a Plasma Therm Batchtop PE/RIE (oxygen plasma, 1 min, 50 W, 250 mTorr) and hard baked at 200 °C for 30 min. Before use all masters were anti-adhesion-treated for 5min with dichlorodimethylsilane by exposing the surfaces to the vapors under a Petri dish cover. The **Fabrication of polydimethylsiloxane (PDMS) pipettes** is illustrated in figure S1.

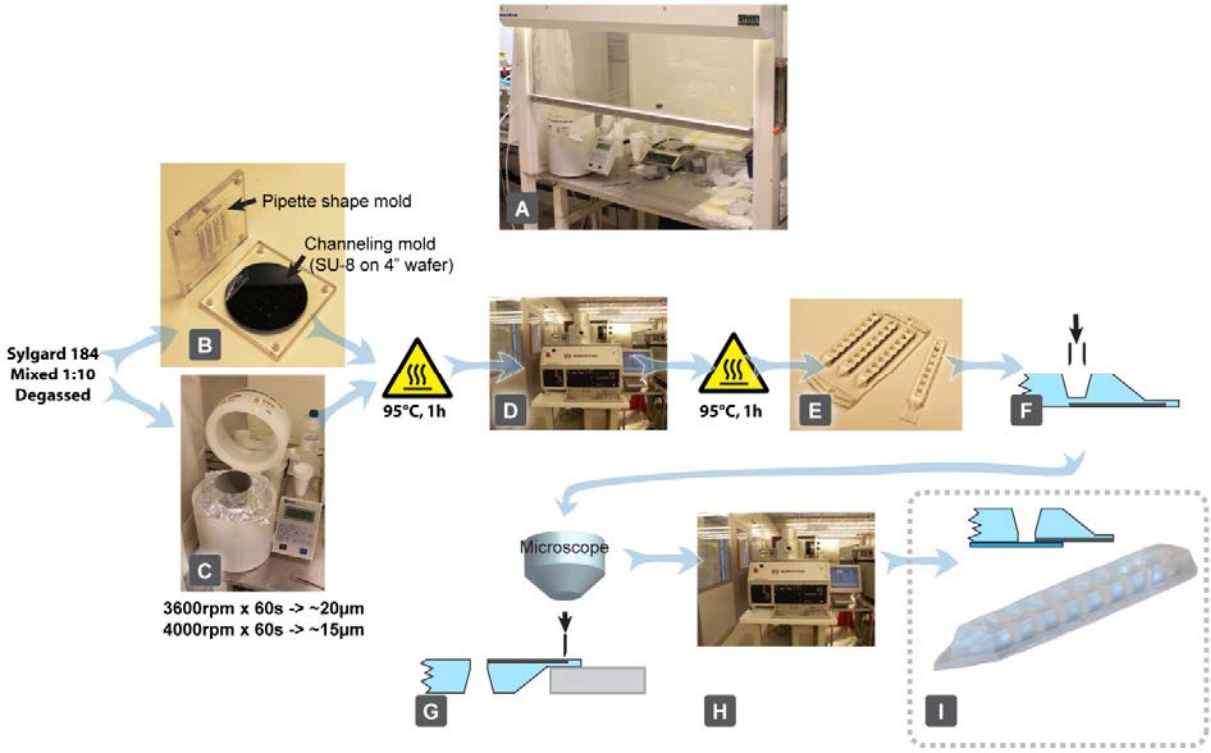

Fig S1. Pipette fabrication by means of replica molding. PDMS casting and curing was performed under a laminar flow hood (A) in a standard laboratory. PDMS pre-polymer (Dow Corning Sylgard 184) was prepared by mixing parts A and B in a ratio 10:1 (wt:wt) and degassed for 15 min in a vacuum desiccator. Subsequently the PDMS mixture was cast into the mold (B). This mold is a combination of a machined polycarbonate upper part, defining the macroscopic shape of the pipettes, and a lower plate supporting a 4" wafer master. The thin PDMS layer was spin-coated onto an unstructured 4" wafer (C). Both parts were cured in an air circulation oven at a temperature of 95°C for 1 h. Thereafter, the slab containing four pipette structures was removed from the mold. Both the slab and the thin PDMS layer, still attached to the wafer, were plasma treated (Plasma Therm Batchtop PE/RIE at 250 mTorr, 85 W, 10 sccm O_2 for 10 s) (D) and bonded to each other, followed by a baking step (95°C for 1h) to strengthen the bonding. The composite slab was then removed from the wafer and the individual pipettes were cut out (E). Subsequently the wells were punched out (F). Honing of the tip shape was performing using a microtome blade while observing the cutting region using a standard inspection microscope (G). Finally, the shaped PDMS part was plasma bonded onto a rectangular glass support (H), resulting in a functional "ready to use" tip (I). The whole process has a high yield and can be easily scaled through the use of larger wafers. Less scalable steps are the manual tip cutting (G), which currently requires individual alignment of the cutting blade and bonding to the glass support (H). It also requires prior alignment of glass and PDMS pieces. However, tools to facilitate or automate these steps are conceivable.

Supplementary figures

Fig S2 (Tube optimization)

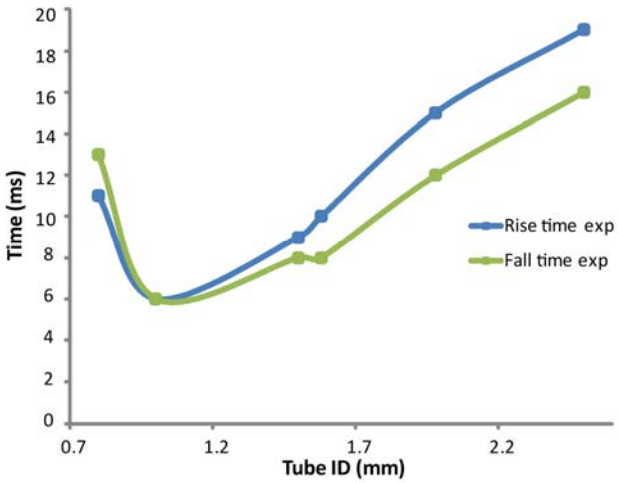

Fig S2. Pressure propagation in supply tubes connecting the valve controller to the manifold, depending on their inner diameter (ID). In order to optimize the fluid switching speed, we compared different tubing materials and internal diameters. All the tubes tested were 1.0 m long. Narrow tubes have higher fluidic resistance hindering gas flow (tube limited), whereas wide tubing has a high volume with lower flow resistance, but needs to be filled (supply limited). For our pump supply, the optimal tube size was found to be 1 mm I.D, exhibiting both exponential rise and fall times of 6 ms. Rise and fall times without tube were measured to be 2 ms, indicating for a 1m section, the tube contributes with 4 ms.

Fig S3 (Pneumatic control system)

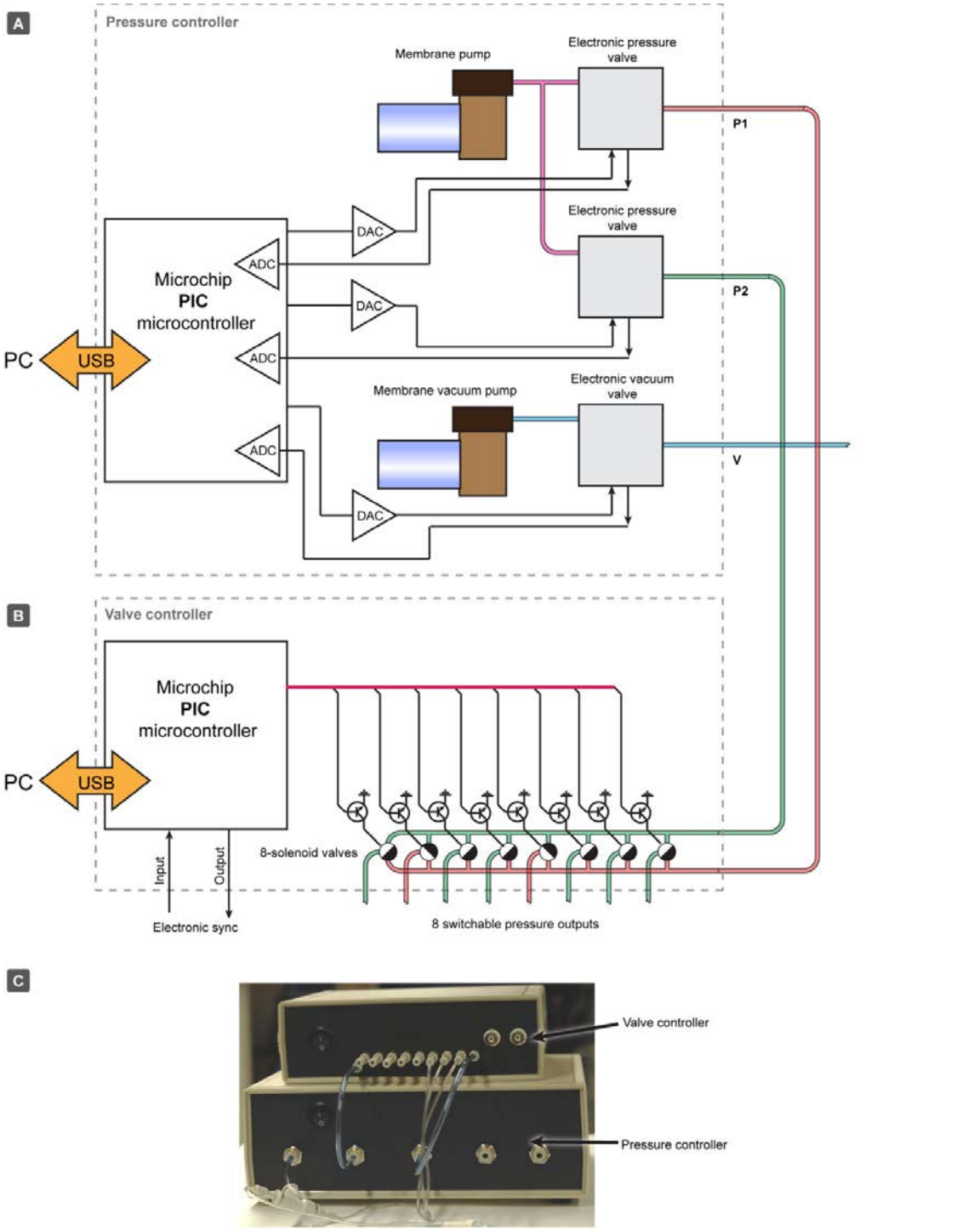

Fig S3. Pneumatic control schematic and assembly. The components were purchased from SMC Sweden (pumps, electronic valves), Pneumadyne Inc. (solenoid valves) and ELFA AB (all other parts). The control unit was divided into two subunits: pressure controller (A) and valve controller (B). The control electronics are based on a PIC18F4550 microcontroller, interfaced to a PC via USB 2.0. Both pneumatic controller subunits (C) were equipped with 4mm push-fit connectors, which allow for quick reconfiguration, depending on the experiment and the type of pipette tip used.

Fig S4 (Tip stability)

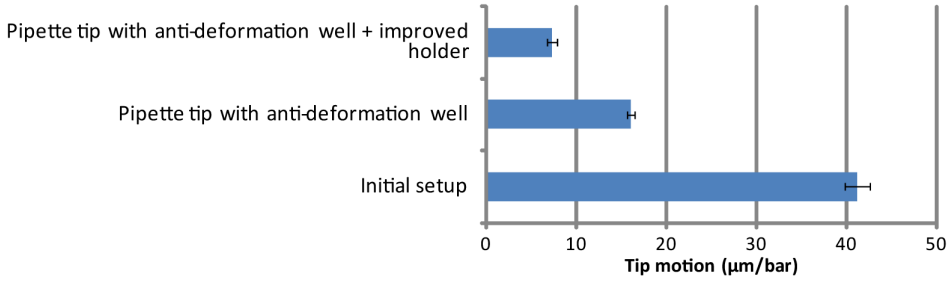

Fig S4. Minimizing tip displacement under operation. Due to material elasticity, the PDMS can deform and cause the pipette tip to change position by several µm when the pressure in the wells is changed. The tip displacement is mostly axial, with respect to the sample. This effect can be comparatively large when the pressure change takes place in the first well, i.e. closest to the tip. In our initial setup we observed elastic displacement of up to 40 µm/bar. Tip displacement can be also caused by deformation of a structurally weak tip holder. To reduce tip motion we added a deformation isolation well and upgraded the holder design to improve its structural strength. After these changes the motion was reduced to ~7 µm/bar. In typical experiments, the pressure steps are < 0.5 bar, yielding positional stability better than 4 µm.

Fig S5 (Single cell solution delivery)

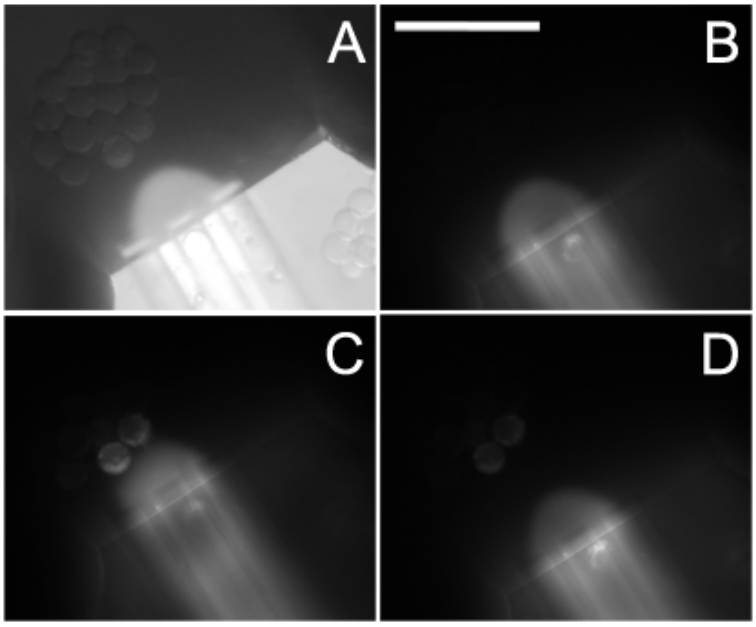

Fig S5. Targeted delivery to individual HEK293 cells by means of the multipurpose pipette. The flow recirculation is maintained throughout the experiment, thus delivery to the cell is controlled through positioning of the pipette tip. A small isolated patch of HEK293 cells adhered to a glass coverslip is approached. Both recirculation volume and cell colony are visible in a combined brightfield and fluorescence image (A). Initially the cells contain no fluorescently labelled species (B). Individual cells from the collective are targeted, and a Rhodamine B solution is delivered to label the cells (C). The label remains inside the cells upon retraction of the pipette. However, progressing photobleaching diminishes the fluorescent signal (D). The scale bar in panel B represents 90 µm.

Supplementary analysis (Solution exchange times)

Here we provide a breakdown of the components contributing to the solution exchange time. Solenoid valves and external tubes were characterized experimentally (Fig. S2).

Inertia

If we change pressures and therefore the flow rates, the liquid has to be accelerated, which happens not instantaneously.

$$A\Delta p = A(p - QR) = \rho V a$$

Where *A* is the cross section area, *p* is applied pressure change, *Q* is the flow rate, *R* is the fluidic resistance of the channel, *ρ* is the density of the liquid, *V* is the volume of the channel and *a* is the average acceleration

$$A(p - QR) = \rho \frac{dQ}{dt}$$

$$\frac{-\rho}{AR}\int_0^q \frac{dQ}{Q - \frac{p}{R}} = \int_0^T dt$$

$$\frac{-\rho}{AR} ln\left(1 - \frac{qR}{p}\right) = T$$

If we consider an exponential rise of the flow rate then $q = (1 - e^{-1})\frac{p}{R}$ and

$$\tau = \frac{\rho}{AR}$$

In our system: $A = 20 \cdot 40 \cdot 10^{-12} m^2 = 8 \cdot 10^{-10} m^2$, $R = 2.8 \cdot 10^{15} \frac{m^3}{s\,Pa}$, $\rho = 1000 \frac{kg}{m^3}$

$$\tau = 0.45\ ms$$

Supply channel

Channel deformation was also studied using COMSOL models for structural mechanics coupled with a moving mesh (Arbitrary Langrangian-Eulerian technique) (Fig. S6). The necessary mechanical parameters of Dow Corning Sylgard 184 PDMS were reported previously (F. Schneider, T. Fellner, J. Wilde, U. Wallrabe, *J. Micromech. Microeng*., 2008, **18**, 065008). As a result, a roughly linear dependence was found between the applied pressure and a subsequent volume increase (at 1 bar the channel volume increases roughly 40%). This gives a specific fluidic capacitance of channel *c*

$$c = \frac{dC}{dl} = 3.2 \cdot 10^{-15} \frac{m^2}{Pa}$$

Fig S6. PDMS channel deformation at an applied internal pressure of 1 bar. The largest channel deformation is directed towards the thin bottom layer. PDMS channels extending into the bulk of the device contribute much less, $c \approx 1 \cdot 10^{-15} \frac{m^2}{Pa}$, but this is harder to estimate accurately due to complex device geometry.

Flow rate propagation in a fluidic RC-line

If we look the channel it is a one dimensional conducting line

$$\frac{L}{R}\frac{dp}{dx} = W = \frac{dQ}{dt}$$

$$\frac{dW}{dx} = \frac{cdp}{dt}$$

$$\frac{L}{Rc}\frac{d^2p}{dx^2} = \frac{dp}{dt}$$

Differential equations with this form are known as diffusion or thermal conductance equations. We can solve it for 1D form in COMSOL. For channels, of which 41mm are in supported and 10mm in unsupported PDMS. This yields a rise time of ~**30 ms**. (Fig. S7)

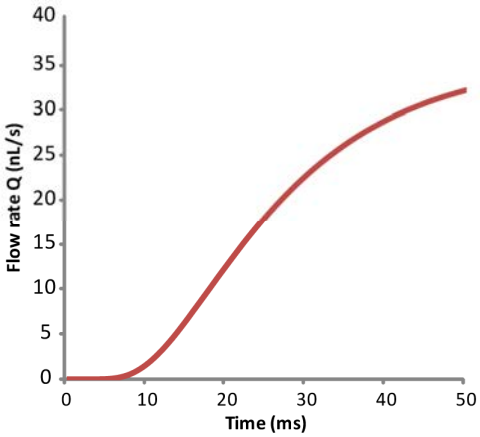

Fig S7. Results of a COMSOL model, estimating the increase of the flow rate at the end of the supply channel after applying a pressure pulse to the entrance to the channel (well).

Dead volume of the switch

For fluid switching to occur, the fluid front has to move over the output channel and a certain volume of the switch cavity has to be filled, requiring fluid flow

$$\tau = \frac{VR}{\Delta p}$$

This volume is ~0.03 nL, which for a pressure step of 0.3 bar results in a contribution to the solution exchange time of ~2.5 ms.

Fluid dispersion in the outlet channel

During the transport of the concentration pulse through the outlet channel, it is subject to dispersion. In our case,

$$Pé \approx \frac{(d/2)v}{D} = 250$$

where $d = 20\mu m$ is the channel dimension, $r \approx d/2$ is the approximate radius, $v = 12.5\, mm/s$ is the average flow velocity corresponding to a flow rate $Q = 5nL/s$ and $D = 5 \cdot 10^{-10}\, m^2/s$ is molecular diffusivity of fluorescein (a good estimate also for other small molecules). In order to choose a suitable dispersion model, we also evaluate the ratio of channel length and radius.

$$\frac{L}{r} = 100$$

This processes is convection dominated ($Pé > 0$), but since $Pé < 10\frac{L}{r} = 1000$, diffusion cannot be neglected. The channel length is not sufficient to establish the Taylor regime ($Pé > 0.4\frac{L}{r} = 40$). The observed more complex regime is located in a transition region on a landscape of dispersion modes, according to R. F. Probstein, *"**Physiochemical Hydrodynamics. 2nd Edition,** ch. 4.6: Taylor Dispersion in a Capillary Tube"*, John Wiley & Sons, 1995. Therefore, the stepwise propagation of solute concentration through the square channel was modeled in COMSOL Multiphysics using a transient convection-diffusion simulation (Fig. S8). The concentration rise times obtained from this simulation were fitted to a power function.

$$\tau \approx 6.728[s] \cdot (L/[m])^{0.657}$$

We can compare this result with Taylor dispersion on one hand

$$\tau = (1 - e^{-1})\sqrt{\pi \frac{d^2 L}{48Dv}} = (1 - e^{-1})\sqrt{\pi \frac{d^4 L}{48DQ}} \approx 0.16 \cdot d^2 \sqrt{\frac{L}{DQ}}$$

and with pure convective dispersion on another hand.

$$\tau \approx 4.21 \frac{L}{v_{max}}$$

Regime	Scaling	Rise time *L=1mm* channel
Taylor dispersion (circular tube)	$\tau \propto d^2 L^{0.5} Q^{-0.5}$	~40 ms
Pure convection (circular tube)	$\tau \propto d^2 L^1 Q^{-1}$	~234 ms
Simulation (square tube)	$\tau \propto L^{0.657}$	70 ms

With respect to both scaling and rise time, the simulated results reside between these two pure regimes, being somewhat closer to the Taylor regime.

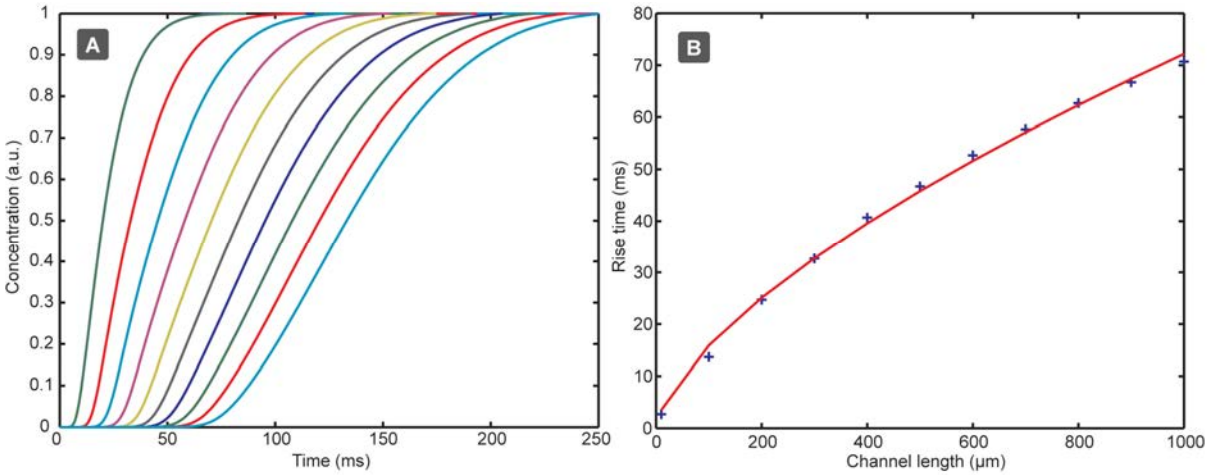

Fig S8. COMSOL Simulation of spreading from a rectangular concentration front, when passing through the output channel. (A) Evaluation for different channel lengths from L = 100-1000 µm. Flow rate Q = 5nL/s. (B) 63 % concentration rise times depending on channel length, fitted with a power function $\tau \approx 6.728[s] \cdot (L/[m])^{0.657}$

Outlet to cell

Solution delivery from the device outlet to the cell or surface is the most difficult to describe and to analytically solve or approximate, due to the complex interplay of recirculating flow, geometry and diffusion. Therefore a numerical COMSOL simulation was performed.

Scaling

We evaluate the scaling laws in dependence on the channel size for constant flow and pressure (Fig. S9)

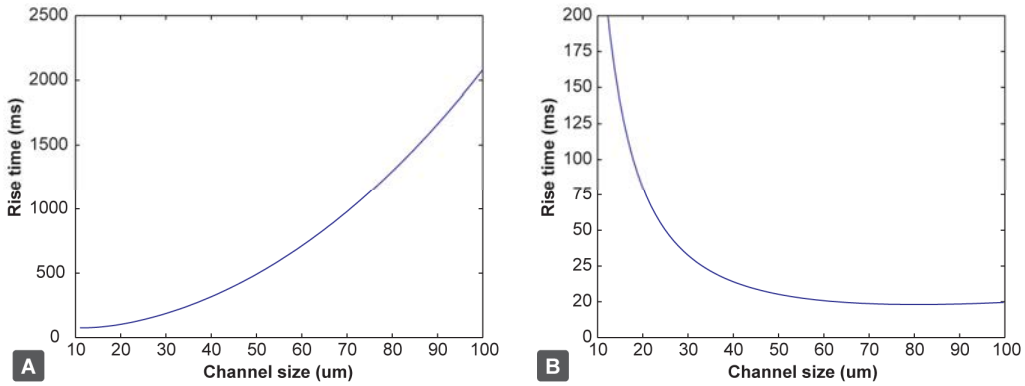

Fig S9. **Scale dependence of the rise times** (Sum of the components of inertia, dead volume, supply channel and output channel, but without external components) on the channel size, in case of constant flow rates (A) and constant pressures (B).

From this analysis we conclude that at constant flow rates small channels are favourable. However, when considering a constant pressure regime, using the same pressure control, a channel size range around 40-60µm could be most suitable for high speed switching. This increase implies that the flow rates are significantly larger (20-80x times), indicating that the integrated wells would be depleted in <1 min. However, this could be a suitable option when designing a device for applying rapid, short pulses.

Captions of supplementary movies

SMovie 1 (Positionable solution exchange)

This movie demonstrates the ability to reposition the flow recirculation zone during solution exchange between three colored liquids (green, yellow and red).

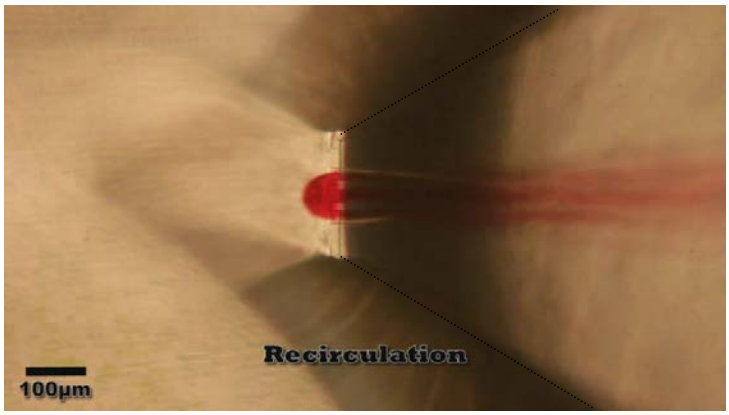

SMovie 2 (Individual cell-targeted delivery)

A small isolated patch of several HEK-293 cells adhered to a glass coverslip are approached by the pipette, and one or two cells are targeted for labeling with a Rhodamine B solution, delivered by the pipette. The recirculation zone is maintained throughout the clip, such that delivery is mediated through positioning. The panels for figure S5 were extracted from this movie.